

# Giant topological magnetoelectric and optical Hall effects for topological insulator as a defect in photonic crystal

Peng Wang, Qin Liu\*, Wei Li, Xunya Jiang†

State Key Laboratory of Functional Materials for Informatics,

Shanghai Institute of Microsystem and Information Technology, CAS, Shanghai 200050, China

(Dated: October 5, 2018)

A system with a topological insulator slab sandwiched by two one-dimensional photonic crystals as a defect is investigated. A giant topological magnetoelectric effect is proposed which is characterized by two resonant peaks with half-unit transmissions and rich polarization behaviors in the photonic band gap. We also predict a giant optical Hall effect in our system, in which the transverse shift of the transmitted light could be thousand times larger than the wavelength. These effects are purely from the  $\Theta$ -domain walls at the topological insulator interfaces and could be observed easily. These effects can also be used as the sensitive detection of basic physical constants.

PACS numbers: 85.75.-d, 78.20.Ls, 73.43.-f, 03.65.Vf

*Introduction.* The modification to the Maxwell Lagrangian of classical electromagnetism by a term,  $\mathcal{L}_a = \frac{\Theta}{2\pi} \frac{\alpha}{2\pi} \mathbf{E} \cdot \mathbf{B}$ , is known as “axion electrodynamics” in field theory literature [1], where  $\alpha = e^2/\hbar c$  is the fine structure constant, and  $\Theta$  is known as the axion field. Novel effects arise when the axion field is a function of space-time [1–3]. Recently it is argued that  $\mathcal{L}_a$  can be realized as the low-energy physics of three-dimensional (3D) topological insulators (TI) [4], which have been theoretically predicted and/or experimentally observed in various binary [5–8] and ternary [9–12] compounds. In this context, the Lagrangian  $\mathcal{L}_a$  describes the topological part for the electromagnetic response of 3D TI with modified constitution equations  $\mathbf{D} = \epsilon \mathbf{E} - \alpha(\Theta/\pi)\mathbf{B}$ ,  $\mathbf{H} = \mathbf{B}/\mu + \alpha(\Theta/\pi)\mathbf{E}$ , where  $\epsilon$  and  $\mu$  are respectively the material permittivity and permeability. In the above,  $\Theta = 0$  or  $(\pm)\pi$  is viewed as a phenomenological parameter which categorizes all time-reversal invariant insulators into  $Z_2$  trivial or non-trivial class. Since the  $\Theta$  term can be written as a total derivative in the Lagrangian, it causes nontrivial effects *only* at the interfaces, which separate TI and normal insulators and are also called as  $\Theta$ -domain walls (DWs). These effects on  $\Theta$ -DWs are known as the topological magnetoelectric effects (TME), in which an electric field can induce a magnetic polarization and a magnetic field can induce an electric polarization. To eliminate the sign ambiguity of  $\Theta$  for  $Z_2$ -nontrivial insulators, a T-breaking surface magnetic field is applied to determine the winding direction of  $\Theta$  through the DW, so that  $\Theta = \pi$  when the magnetization is in the interface normal direction and  $-\pi$  when the magnetization is inverted.

As a direct consequence of  $Z_2$  nontriviality, great attentions have been focused on the TME [13–16], among which one [13] abandons the toy semi-infinite geometry

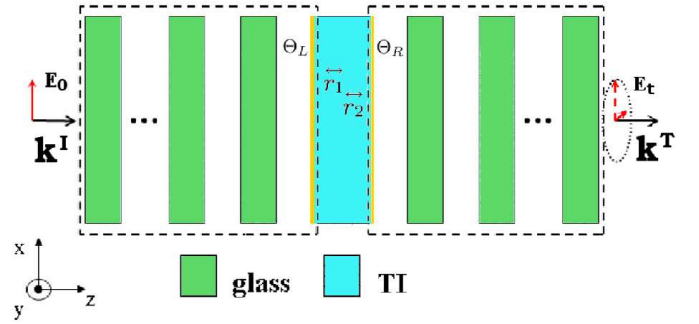


FIG. 1: Schematic show of our model with a TI slab as defect sandwiched by two 1D PhCs.

and seriously considers the realistic thin-film structure of TI [17] as well as the weak exchange-coupling to the surface magnetization. In this connection, optical methods take special advantages in measuring the TME experimentally [18, 19], *e.g.* by measuring the Kerr or Faraday rotation angles,  $\theta(\mathbf{B})$ , in the zero  $\mathbf{B}$ -field limit. However, TME is very weak generally since  $\theta(B \rightarrow 0^+) \propto \alpha$  and has not been observed experimentally so far, hence, finding larger physical effects to manifest  $Z_2$  nontriviality is very essential.

Motivated by these facts, in this letter, we study the transmission characteristics of a system with a 3D TI slab sandwiched by two 1D photonic crystals (PhCs) as a defect using the standard transfer-matrix method (TMM) [20]. It is found that, there are *two* resonant peaks in the photonic band gap (PBG) with half-unit transmission each, which is in sharp contrast with a single unimodular resonant peak of a normal defect. For normal incidence with linear polarization, the transmitted waves at the two resonant peaks are left and right circular polarized respectively, and at the central frequency between the two peaks, the polarization of the transmitted wave

\*liuqin@mail.sim.ac.cn

†xyjiang@mail.sim.ac.cn

is linear but with the Faraday rotation angle about  $\pi/2$ . These diverse phenomena play the role of “giant TME” and can be optically detected at Terahertz (THz) for real TI materials. Moreover, with small incident angle, a giant transverse shift, which could be thousand times larger than wavelength, is predicted for the resonant transmitted light, which is termed as “giant optical Hall effect” [21, 22] in this work.

*Our system*, as shown in Fig.1, is made of a FM-TI-FM heterostructure and two symmetric N-cell 1D PhCs at both sides. Each cell consists of a glass and a vacuum layer. The surface FM magnetization in  $z$ -direction generally could be parallel and antiparallel [4], in which the  $\Theta$ -DWs at the left and right surfaces of the TI are respectively  $(0, \pi)$ - $(-\pi, 0)$  and  $(0, \pi)$ - $(\pi, 0)$ . The FM layer opens an energy gap of the surface states of TI, which is typically  $E_g = 10$  meV [4]. Since the effective theory  $\mathcal{L}_a$  applies only in the low frequency limit,  $\omega \ll E_g/\hbar$ , which implies that the working frequency of interest is within THz range, to detect the topological phenomena, the refractive indexes and the thickness for the binary PhC cell and the TI slab are taken respectively as  $n_g = 1.5$ ,  $n_v = 1.0$ ,  $n_{TI} = 10$ , and  $d = d_g = d_v = d_{TI} = 0.1$  mm. Under this choice, the central frequency of the first PBG is around 0.6 THz, and the finite size effect of the TI defect can be neglected [23].

*Giant topological magnetoelectric effect.* As the starting point, we first consider the parallel magnetization case where  $\Theta_L = -\Theta_R = \pi$ . The transmission spectrum with PhC cell number  $N = 10$  for a normally incident linear plane wave with  $\mathbf{E}_0$  along  $x$ -axis is shown in Fig.2(a). Surprisingly, two topological-defect resonant peaks are observed with half-unit transmission each. We have also checked other cell numbers and the evolution of peaks with  $N$  is shown in Fig.2(b). It is found that when  $N \leq 5$ , there is a single almost-unimodular resonant peak in PBG, with increasing  $N$ , the single peak splits into two, which turn to be so sharp that they are well-separated when  $N > 7$ . Furthermore, at  $N = 10$ , the polarization of the transmitted light changes from right ( $\omega_1$ ) to left elliptic ( $\omega_5$ ) with the frequency increasing as in Fig.2(c). There are three frequencies at which the polarizations are of particular interests. At two resonant frequencies  $\omega_2$  and  $\omega_4$ , the transmitted lights are of right and left circular polarization respectively, while at the central frequency  $\omega_3$  between them, the transmitted light is linearly polarized again but with a giant Faraday rotation angle about  $\pi/2$ .

To understand these anomalous phenomena of topological defect in PhC, we set up a simple Fabry-Perot (FP) cavity model for our system. As shown in Fig.1, if we take the areas in the two dashed boxes (which include the  $\Theta$ -DWs at the surfaces of the TI slab and PhC) separately as left and right effective mirrors, then the system can be treated as a typical FP cavity. Before taking deeper insight into the TI FP cavity, we first review the theory

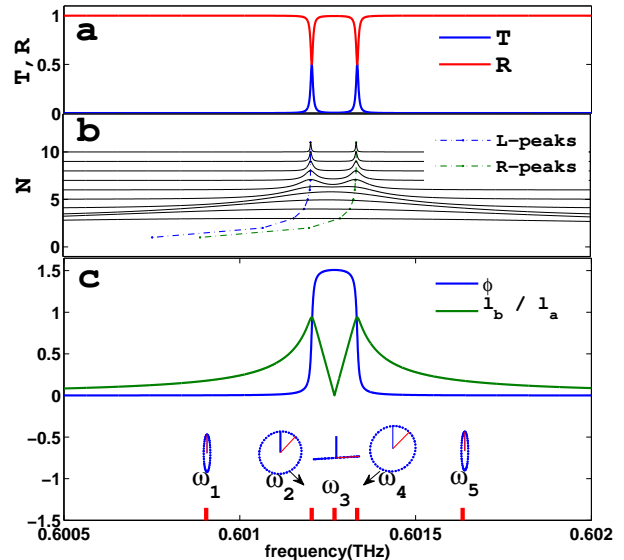


FIG. 2: (a) Transmission  $I_t/I_i$  and reflection  $I_r/I_i$  spectra with incidence as a linearly-polarized plane wave. (b) Evolution of transmission peaks with cell number  $N$ . The solid lines are numerical results, while the dash-dots are from our theoretical resonant conditions. (c) Angle  $\phi$  (blue line) between the long-axis of polarization and  $x$ -axis, and the intensity ratio (green line) between the short- and long-axis  $l = I_b/I_a$  as a function of frequency. The insets are schematic polarization of transmitted wave at five typical frequencies, where the long-axis is shown in red.

of a conventional one [20]. For a FP cavity with *conventional* material, the transmission coefficient for the FP cavity is well-known as  $t_{FP} = t_1 t_2 e^{ik_z d} / (1 - r_1 r_2 e^{2ik_z d})$ , where  $t_1$ ,  $r_1$  and  $t_2$ ,  $r_2$  are respectively the left-to-right transmission and reflection coefficients of the two mirrors, and  $k_z d$  is the one-way optical path through the cavity. This FP transmission coefficient is usually pictured as the sum of all orders back-forward scattering between the two mirrors,  $t_{FP} = t_1 t_2 e^{ik_z d} [1 + r_1 r_2 e^{2ik_z d} + (r_1 r_2 e^{2ik_z d})^2 + \dots]$ , from which we see that the resonant condition  $\phi_{r_1} + \phi_{r_2} + 2k_z(\omega)d = 2m\pi$ ,  $m \in \mathbb{N}$ , is satisfied simultaneously for both TM =  $(1 \ 0)^T$  and TE =  $(0 \ 1)^T$  modes, where  $r_{1,2} = |r_{1,2}| \exp(i\phi_{r_{1,2}})$ . Therefore there is one single resonant peak in transmission spectrum with unit transmission  $T_{FP} = |t_{FP}|^2$ .

However for a TI FP cavity, the above theory needs to be modified due to the existence of  $\Theta$ -DWs. In previous studies [4, 13, 18], nonzero Kerr or Faraday rotations at  $\Theta$ -DWs are predicted, where waves of different linear polarization couple to each other. This fact tells us that the TM and TE modes are *no* longer good bases in the presence of  $\Theta$ -DWs, and in these bases, the reflection

(transmission) properties are described by a 2 by 2 matrix, termed as “reflection (transmission) matrix”  $\overleftrightarrow{r} \left( \overleftrightarrow{t} \right)$ . Therefore, to obtain the resonant condition following the same discussions as the above, the key question is: what are the good bases for systems with  $\Theta$ -DWs? This problem is resolved by finding the form of  $\Theta$ -DW reflection (transmission) matrix as:

$$\overleftrightarrow{r} \left( \overleftrightarrow{t} \right) = \begin{pmatrix} A_{r(t)} & B_{r(t)} \\ -B_{r(t)} & A_{r(t)} \end{pmatrix}, \quad (1)$$

where  $A_{r(t)}$  and  $B_{r(t)}$  are real, and the off-diagonal term generated by the  $\Theta$ -DW,  $B \propto \alpha$ , is a small value. The good bases of such matrix are nothing else but  $\sigma_{\pm} = (1 \mp i)^T / \sqrt{2}$ , which are respectively the right and left circular polarized waves. Physically this means, if we normally incident one eigenmode of  $\overleftrightarrow{r}$ , say  $\sigma_+$ , then the reflected wave is still  $\sigma_+$  but multiplied by a reflecting coefficient  $r_{DW} = |r_{DW}| \exp(i\phi_{DW})$ , where  $|r_{DW}| = (A_r^2 + B_r^2)^{1/2} \sim |A_r|$  and  $\phi_{DW} = \arctan(-B_r/A_r)$  is a topological phase generated by  $\Theta$ -DW. For our TI FP cavity where each effective mirror includes not only a  $\Theta$ -DW but also a PhC, the essential tricky is that the reflection (transmission) matrix of such mirrors still has the form of Eq.(1), but with  $A_r = |A_r| \exp(i\phi_r)$  being a complex number and  $\phi_{DW} = \arctan[\Re(-B_r/A_r)]$ . Therefore,  $\sigma_{\pm}$  are still good bases and any normal incident wave could be expanded as  $\mathbf{E}_0 = (E_+ \sigma_+ + E_- \sigma_-) / \sqrt{2}$ , where  $E_{\pm} = E_x \pm iE_y$ , so the discussions for a conventional FP cavity are valid separately for each basis of  $\sigma_{\pm}$ , and the transmission of our system is  $T_{FP} = \frac{1}{2} \sum_{s=\pm} \frac{(1-R)^2}{(1-R)^2 + 4R \sin^2 \left( k_z d + \phi_r + s \frac{\phi_{DW_1} + \phi_{DW_2}}{2} \right)}$ ,

where  $R = |A_r|^2 + |B_r|^2$ . Obviously, the theoretical resonant conditions for  $\sigma_{\pm}$  modes are:

$$2k_z(\omega)d + 2\phi_r \pm (\phi_{DW_1} + \phi_{DW_2}) = 2m\pi, \quad m \in \mathbb{N}. \quad (2)$$

The phases  $\pm(\phi_{DW_1} + \phi_{DW_2})$  generated by two  $\Theta$ -DWs lead to *two* resonant frequencies  $\omega_{2,4}$  for  $\sigma_{\pm}$  modes. In Fig.2(b), we plot the resonant frequencies obtained by Eq.(2) for different  $N$  in dash-dots, which is compared with those obtained by numerical methods shown in solids, and we see that they agree with each other very well. Two essential properties are concluded. First, the PhCs are crucial to observe the double peaks due to their narrowing down peakwidth dramatically. Second, the frequency difference between the two peaks,  $\delta\omega = \omega_4 - \omega_2$ , is almost a constant as the change of  $N$ , although the two resonant peaks are unsolvable in spectra for small  $N$ . Actually, even without PhCs, the resonant condition Eq.(2) still gives two resonant frequencies for a bare TI slab, so the two-peaks spectrum is an intrinsic property generated by  $\Theta$ -DWs. For our system, it is found that  $\delta\omega/\omega \simeq \frac{4n_{TI}}{(n_{TI}^2 - n_0^2)} \alpha$ . Since experimentally we can measure the frequency almost exactly by interferometers,  $\delta\omega$

is a new way not only to manifest topological nontriviality but also to measure the basic physical constant  $\alpha = e^2/\hbar c$ .

In Fig.2(c), a rich behavior of polarization is shown versus frequency, which can also be understood in the TI FP cavity model. At resonant frequency,  $\omega_2$  or  $\omega_4$ , only one eigenmode is totally transmitted while the other is totally reflected, so the total transmitted light is circular polarized. While at  $\omega_3$  the transmission amplitudes of both  $\sigma_{\pm}$  modes are small but the same, so that the total transmitted wave is linearly polarized again, but with the Faraday rotation angle about  $\pi/2$  (or  $3\pi/2$ ).

In contrast, if the TI slab has antiparallel magnetization at two interfaces with  $\Theta_L = \Theta_R = \pi$ , the TI FP cavity goes back to a conventional one with a single unimodular resonant peak. This is because in this case,  $A_{r_1} = A_{r_2}$  while  $B_{r_1} = -B_{r_2}$ , so that  $\phi_{DW_1} = -\phi_{DW_2}$  and Eq.(2) recovers that of the conventional FP cavity. Unlike the parallel magnetization case where the Faraday rotation is doubled when light passes two  $\Theta$ -DWs from left to right, for antiparallel magnetization, the opposite half-quantized Hall conductances carried by the two surfaces cancel each other, hence there is no net Faraday rotation when out of the TI defect. Vanishing of TME in antiparallel case is another demonstration of pure  $Z_2$ -nontriviality effect of our system. For experimentalists, antiparallel case is also a way to eliminate systematic errors.

*Giant optical Hall effect (OHE) of TI defect.* In electronic systems, the anomalous velocity ( $\mathbf{k} \times \mathbf{\Omega}_k$ ) originating from Berry curvature  $\mathbf{\Omega}_k$  [24, 25] in various Hall effects has been well studied [26–28]. In parallel Onoda *et al.* construct in Refs. [21, 22] a theory for the propagation of an optical wave packet in slowly-varying photonic systems, such as chirped PhC. A set of general equations of motion (EOM) is derived in the adiabatic limit, from which the anomalous velocity is proved to be consistent with a more basic physical requirement, i.e., the total angular momentum conservation (TAMC). The nonvanishing anomalous velocity predicts many interesting dynamical phenomena, one of them is the OHE which could be measured by a transverse shift of the transmitted light beam at the interface between different media as shown in Fig.3(a). Strictly speaking, the EOM is not applicable for sharp change at interface due to the failure of the adiabatic condition, however the correct beam-shift value can be obtained by the TAMC law. Generally, the transverse shift in OHE is only a fraction of the wavelength. A kind of *giant* OHE, where the transverse shift is thousand times of the wavelength (or  $10^6$  atomic lattice constant), is predicted at the interface between a PhC and vacuum when a small PBG  $\Delta$  is opened at the original Dirac point by spatial-inversion symmetry breaking [21, 22]. The mechanism of the giant OHE is understood by TAMC such that a very strong pseudo-spin of Bloch function in PhC needs to be compensated by the orbital

angular momentum in vacuum in the form of large transverse shift.

In our system, we report a completely different mechanism to generate the giant OHE. Before getting into the details, let's first go over the calculations of the OHE transverse shift at interface by TAMC [21, 22]. For a system with rotational symmetry around the  $z$ -axis, the  $z$ -component of the total angular momentum with both orbital and "spin" (including pseudo-spin of the Bloch function) degree of freedoms,  $j_z = [\mathbf{r}_c \times \mathbf{k}_c + \langle z_c | \sigma_z | z_c \rangle (\mathbf{k}_c / k_c)]_z$ , is conserved between incident and transmitted lights,  $j_z^I = j_z^T$ . Here  $\mathbf{r}_c$  and  $\mathbf{k}_c$  are respectively the central position and wavevector,  $|z_c\rangle$  is a two-component spinor and  $\sigma_z$  is the Pauli matrix. The TAMC yields the transverse shift for the central position of transmitted light beam as [21, 22]:

$$\delta y_c^T = \frac{1}{k_c^I \sin \theta_I} [\langle z_c^T | \sigma_3 | z_c^T \rangle \cos \theta_T - \langle z_c^I | \sigma_3 | z_c^I \rangle \cos \theta_I], \quad (3)$$

where  $\theta_{I(T)}$  is the angle between the  $z$ -axis and  $\mathbf{k}_c^{I(T)}$  of the incident (transmitted) light. From Eq.(3), the giant OHE at PhC-vacuum interface [21, 22] can be explained by the vanishing of the large PhC pseudo-spin,  $\langle z_c^I | \sigma_3 | z_c^I \rangle \propto 1/\Delta^2$ , which diverges at the limit  $\Delta \rightarrow 0$ . For our system, if we choose a linearly-polarized *nearly-normal* incident beam with frequency at the resonant one,  $\omega_2$  or  $\omega_4$ , the transmitted light (with half-unit transmission) is right or left circularly polarized, which means that  $|\langle z_c^T | \sigma_3 | z_c^T \rangle \cos \theta_T - \langle z_c^I | \sigma_3 | z_c^I \rangle \cos \theta_I| \simeq |\pm 1 - 0| = 1$  is almost a constant at small incident angles. However,  $\delta y_c^T$  diverges since the denominator is approximately  $1/(k_c^I \theta_I) \rightarrow \infty$  in the limit  $\theta_I \rightarrow 0$ .

Using the TMM, the transmission and reflection fields under tilt incidence are also obtained, and  $\delta y_c^T$  as a function of  $\theta_I$ , calculated from Eq.(3), is plotted in Fig.3(b) where its divergence at small incident angles is clearly seen.

Finally, it is interesting to discuss the physical limit for observing giant TME and OHE in our system. From the peakwidth of the resonant modes in Fig.2(a), we note that the modern high quality lasers and interferometers, whose frequency deviation is in order of  $10^{-5}$ , can easily catch the exact resonant frequencies  $\omega_{2(4)}$  of our system, therefore giant TME can be observed. For giant OHE, the limit is not from the frequency regime, but mainly from the  $\mathbf{k}$  regime. To observe the beam shift, the incident beam must have a finite-width  $D_b$ , which is composed of different wavevectors. Suppose the incident beam is a Gaussian one, the distribution width of the wavevectors is  $\Delta k \simeq 1/D_b$ , which determines the minimum-achievable incident angle as  $\theta_I^{min} \simeq \Delta k / k_c$ . Therefore the transverse shift has the magnitude of the beam width  $\delta y \sim 1/(k_c^I \theta_I) \sim D_b$ , which could be nearly hundred or thousand times larger than the wavelength in the laboratory conditions for THz waves. Another way

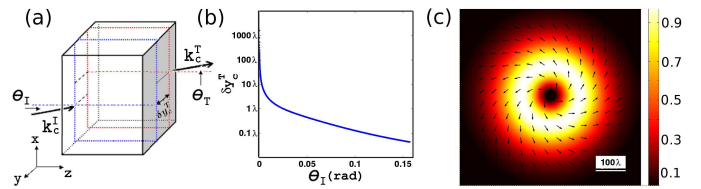


FIG. 3: (a) Schematic show of OHE with transverse shift of transmitted beam. (b) Transverse shift versus incident angle at frequency  $\omega_2$  for our system. (c) The spatial distribution intensity  $I(x, y)$  and the energy current direction of transmitted light when the incidence is a linearly-polarized Gaussian beam with width  $D_b = 100\lambda$  and frequency as  $\omega_2$  in Fig.2.

to directly observe giant OHE is to detect the transmitted beam of a *normally* incident Gaussian beam to our system. Since the nearly-exact-normal  $k$ -components of Gaussian beam have large OHE shift, we expect that the transmitted "beam" is a "light ring" whose center is dark and the maximum should shift to the position nearly  $D_b$  from the beam center as discussed above. Furthermore, since OHE is a *transverse* shift relative to incident interface, the energy current of transmitted beam should have the vortex form. Based on strict Green's function method, we have calculated the transmitted beam of an incident Gaussian beam with width as  $D_b = 100\lambda = 5$  cm and the results are shown in Fig.3(c), which agrees with our expectation very well. Our discussion of both giant TME and OHE can also be applied to the reflected waves. At last, we note that the giant TME and OHE can be utilized not only as manifestation of topological non-triviality, but also as sensitive detecting methods with promising potentials since the simplicity of our system.

*Acknowledgement.* This work is supported by the NSFC (Grant No. 11004212, 10704080, 60877067 and 60938004) and the STCSM (Grant No. 08dj1400303).

- 
- [1] F. Wilczek, Phys. Rev. Lett. **58**, 1799 (1987).
  - [2] E. Witten, Phys. Lett. B **86**, 283 (1979).
  - [3] P. Sikivie, Phys. Lett. B **137**, 353 (1984).
  - [4] X.-L. Qi, T.L. Hughes, and S.-C. Zhang, Phys. Rev. B **78**, 195424 (2008).
  - [5] L. Fu and C. Kane, Phys. Rev. B **76**, 045302 (2007).
  - [6] H. Zhang, C. Liu, X. Qi, X. Dai, Z. Fang, and S. Zhang, Nat. Phys. **5**, 438 (2009).
  - [7] Y. Xia *et al.*, Nat. Phys. **5**, 398 (2009).
  - [8] Y.L. Chen *et al.*, Science **325**, 178 (2009).
  - [9] BH Yan *et al.*, Europhys. Lett. **90**, 546 37002 (2010).
  - [10] H. Lin *et al.*, Nature Materials **9**, 546 (2010).
  - [11] S. Chadov *et al.*, Nature Materials **9**, 541 (2010).
  - [12] D. Xiao *et al.*, Phys. Rev. Lett. **105**, 096404 (2010).
  - [13] Wang-Kong Tse and A.H. MacDonald, Phys. Rev. Lett. **105**, 057401 (2010).
  - [14] X.-L. Qi, R. Li, J. Zang, and S.-C. Zhang, Science **323**,

- 1184 (2009).
- [15] R. Li, J. Wang, X.-L. Qi, and S.-C. Zhang, Nat. Phys. **6**, 284 (2010).
- [16] G. Rosenberg and M. Franz, Phys. Rev. B **82**, 035105 (2010).
- [17] Yao-Yi Li *et al.*, arxiv:cond-mat/0912.5054 (2009).
- [18] M.-C. Chang and M.-F. Yang, Phys. Rev. B **80**, 113304 (2009).
- [19] A.D. LaForge *et al.*, Phys. Rev. B **81**, 125120 (2010).
- [20] Amnon Yariv and Pochi Yeh, *Photonic: Optical electronics in modern communication* (Oxford University Press, 2007).
- [21] M. Onoda, S. Murakami, and N. Nagaosa, Phys. Rev. Letts. **93**, 083901 (2004); Phys. Rev. E **74**, 066610 (2006).
- [22] M. Onoda, S. Murakami, and N. Nagaosa, Phys. Rev. E **74**, 066610 (2006).
- [23] B. Zhou, H.-Z. Lu, R.-L. Chu, S.-Q. Shen, and Q. Niu, Phys. Rev. Lett. **101**, 246807 (2008).
- [24] M.V. Berry, Proc. R. Soc. London A **392**, 45 (1984).
- [25] A.Bohm, A.Mostafazadeh, H.Koizumi, Q.Niu, and J.Zwanziger, *The Geometric Phase in Quantum Systems* (Springer-Verlag,Berlin, 2003).
- [26] Z. Fang *et al.*, Science **302**, 92 (2003).
- [27] M. Kohmoto, Ann. Phys. **160**, 343 (1985).
- [28] S. Murakami, N. Nagaosa, and S.-C. Zhang, Science **301**, 1348 (2003).